Local neurodynamics as a signature of cortical areas: new insights from sleep

Karolina Armonaite[1,2], Lino Nobili[3,4], Luca Paulon[2], Marco Balsi[5], Livio Conti[6,7], Franca Tecchio (iD)[2,1,*]

[1]Faculty of Psychology, Uninettuno University, Corso V. Emanuele II, n. 39, 00186, Rome, Italy,
[2]Laboratory of Electrophysiology for Translational NeuroScience (LET'S), Institute of Cognitive Sciences and Technologies - Consiglio Nazionale delle Ricerche, Via Palestro, n. 32, 00185, Rome, Italy,
[3]Child Neurology and Psychiatry, IRCCS Istituto Giannina Gaslini, Via Gerolamo Gaslini, n. 5, 16147, Genoa, Italy,
[4]Department of Neurosciences, Rehabilitation, Ophthalmology, Genetics and Maternal and Child Health (DINOGMI), University of Genoa, Largo Paolo Daneo, n. 3, 16132, Genoa, Italy,
[5]Department of Information Engineering, Electronics and Telecommunications, Sapienza University, Via Eudossiana, n. 18, 00184, Rome,
[6]Faculty of Engineering, Uninettuno University, Corso V. Emanuele II, n. 39, 00186, Rome, Italy,
[7]INFN – Istituto Nazionale di Fisica Nucleare, Sezione Roma Tor Vergata, Via della Ricerca Scientifica, n.1, 00133, Rome, Italy
*Corresponding author: LET'S—ISTC—CNR, via Palestro 32, 00185 Rome, Italy. Email: franca.tecchio@cnr.it

Sleep crucial for the animal survival is accompanied by huge changes in neuronal electrical activity over time, the neurodynamics. Here, drawing on intracranial stereo-electroencephalographic (sEEG) recordings from the Montreal Neurological Institute (MNI), we analyzed local neurodynamics in the waking state at rest and during the N2, N3, and rapid eye movement (REM) sleep phases. Higuchi fractal dimension (HFD)—a measure of signal complexity—was studied as a feature of the local neurodynamics of the primary motor (M1), somatosensory (S1), and auditory (A1) cortices. The key working hypothesis, that the relationships between local neurodynamics preserve in all sleep phases despite the neurodynamics complexity reduces in sleep compared with wakefulness, was supported by the results. In fact, while HFD awake > REM > N2 > N3 ($P < 0.001$ consistently), HFD in M1 > S1 > A1 in awake and all sleep stages ($P < 0.05$ consistently). Also power spectral density was studied for consistency with previous investigations. Meaningfully, we found a local specificity of neurodynamics, well quantified by the fractal dimension, expressed in wakefulness and during sleep. We reinforce the idea that neurodynamic may become a new criterion for cortical parcellation, prospectively improving the understanding and ability of compensatory interventions for behavioral disorders.

Key words: complexity; neurodynamics; fractal dimension; sleep; cortical parcels.

Introduction

Increasing evidence suggests that distinct cortical parcels can exhibit individual properties of neurodynamics in terms of power spectral density (PSD; Lopes Da Silva 2011; Nobili et al. 2011; Frauscher et al. 2018; Gorgoni et al. 2021) but also different complexity levels (Cottone et al. 2017; Marino et al. 2019; Collantoni et al. 2020; Schartner et al. 2020; Armonaite et al. 2021; Olejarczyk et al. 2022).

Concurrent with the reduction of responsiveness (Andrillon et al. 2016), the complex patterns of the neural activity strongly change when the brain is asleep, with the low frequency waves replacing higher ones prevalent in awake state (Steriade et al. 1993). Underlying specific mechanisms suggest that the neural ongoing electrical activity in sleep is strongly organized and highly regulated (Moruzzi and Magoun 1949; Axmacher et al. 2006; Gent et al. 2018). Such neuronal correlates of sleep mediate its crucial role in strengthening and integrating the 3 controlling systems of the body–brain, the nervous system living in continuous interaction with the hormonal and immunity systems (Steinman 2004; Zhang et al. 2020).

We tested the working hypothesis that, if the local neurodynamics expresses the structure and connectivity of the generating neuronal pools, the differentiation between areas will emerge in sleep stages as well as in awake state (Cottone et al. 2017; Armonaite et al. 2021), despite the changes in the complexity of the brain activity occurring across sleep cycle (Burioka et al. 2005; Casali et al. 2013; Croce et al. 2018; Olejarczyk et al. 2022). Specifically, we investigated in awake and 3 sleep stages (N2, N3, and rapid eye movement [REM]) the local neurodynamics of primary motor (M1), somatosensory (S1), and auditory (A1) cortices, testing whether the relationship of their complexity measured by Higuchi fractal dimension (HFD) maintains the M1 > S1 > A1 in all states, despite the complexity of all areas reduced with sleep depending. To allow comparison with previous investigations, PSD was also assessed.

Previous results about the HFD in M1 and S1 (Cottone et al. 2017; Armonaite et al. 2021) showed that in the 2 areas HFD values largely overlap in the population, so that sampling the 2 areas randomly in different individuals would cancel out the clear differentiation that emerges at the intra-individual level. Also the recent
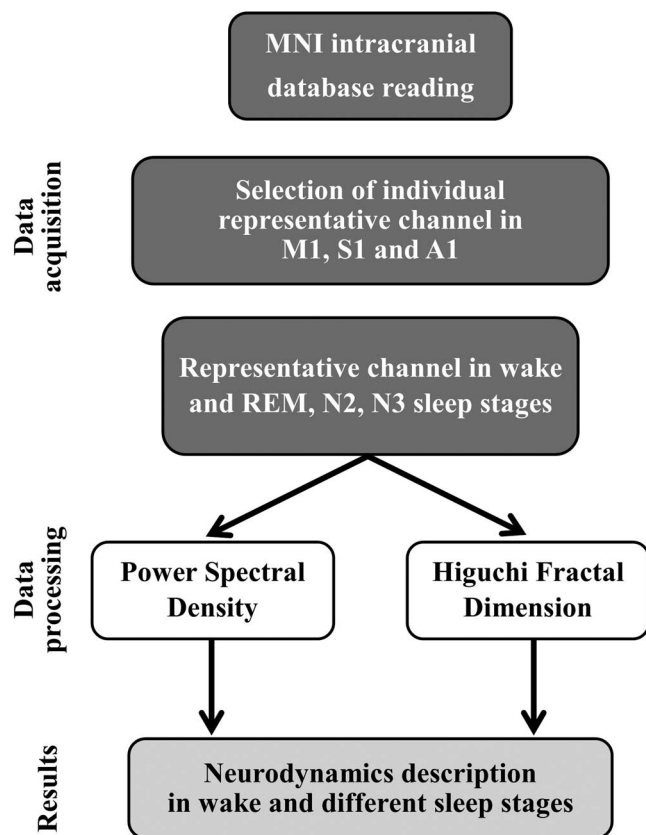
Fig. 1. Study flowchart.

work of Olejarczyk et al. (2022) confirmed that by averaging on the complete Montreal Neurological Institute (MNI) population in the diverse sleep stages the HFD in frontal and parietal areas did not differ statistically. As it is precisely our aim to describe the relationships between the neurodynamics characteristics of the different regions, we have consequently executed the present investigation as an intra-individual analysis.

Materials and methods

The intracranial stereo-electroencephalographic (sEEG) of the MNI public dataset provide recordings from brain regions considered in physiological conditions of patients suffering from drug resistant focal epilepsy (see also section "Limitation of the study").

Data selection

The signals from M1, S1, and A1 primary cortices were studied in 3 sleep stages and wakefulness selecting data from subjects who had at least 2 investigated areas in order to execute the desired strategy of intra-individual analysis (Fig. 1). Briefly reporting the procedure detailed in Armonaite et al. (2021), from the regions of interest (ROIs) we selected one single representative sEEG channel for those available in each subject on the basis of position criteria through the spatial coordinates provided in MNI data. For S1 and M1 the criterion was local proximity, so to have corresponding counterparts of the

same body part representation. For A1, the representative channel was the most central among those available. We obtained 16 subjects in M1, 14 in S1, and 6 in A1 during awake as well as in N2 and N3 sleep stages. The number of subjects was reduced in REM sleep, due to the lack of data, to 13 subjects in M1, 11 subjects in S1, and 5 subjects in A1 (Fig. 2, Supplementary Fig. 2a).

Sleep stage description

The visual scoring of the sleep stages according to the scalp EEG criterion suggested by American Academy of Sleep Medicine, was used by the developers of the MNI dataset. Briefly, 2 EEG derivations were used (Fz–Cz, Cz–Pz according to International 10–20 system). When electrooculogram (EOG), evaluated with an electrode for each eye, and electromyogram for chin muscle were available, REM sleep was identified (von Ellenrieder et al. 2020).

Data provided by MNI was ready for analysis as the recordings of 3 sleep stages were separated as well as each channel was pre-processed by applying low band-pass filter up to 80 Hz and mean subtracted. Each stage was described via 60-s long recordings sampled at 200 Hz.

Neurodynamics—power Spectrum density features

For each channel we calculated the PSD with fast Fourier transform (FFT), by applying the Welch method, with 50% superimposed sliding window, on time series of 256 samples each, tapered with Hamming window. Obtained values of PSD were normalized so that the area under the curve is equal to 1.

Due to the 80 Hz low pass-band filtering of MNI data, we can assess spectral features only up to this frequency value. Frequency spectrum was sub-divided into distinct bands: delta [$\leq$3 Hz], theta [4–7 Hz], alpha [8–12 Hz], low beta [13–25 Hz], high beta [26–32 Hz], low gamma [33–48 Hz], and high gamma [49–80 Hz]. We estimated the mean value of the PSD in each frequency band as the integral divided by the number of frequency bins in the band.

Neurodynamics—fractal features

We hypothesize that fractal analysis can spot the specificities of the neuronal ongoing electrical activity better than linear spectral analysis. Having Cottone et al. (2017) with EEG on the scalp and Armonaite et al. (2021) with intracranial sEEG demonstrated that HFD can estimate the distinctions between cortical parcels in wakefulness, we deployed the same method here, in order to verify whether such HFD feature will persist or vary across 3 sleep stages. HFD is a relatively simple measure of fractal features, yet sensitive in extracting valuable information from physiological time series (Klonowski 2002) and suitable for catching the non-linearity of the underlying processes. Moreover, HFD is a measure derived directly from the time series, avoiding phase representation, relatively independent of the signals' amplitude and length, which could represent an advantage with respect to other
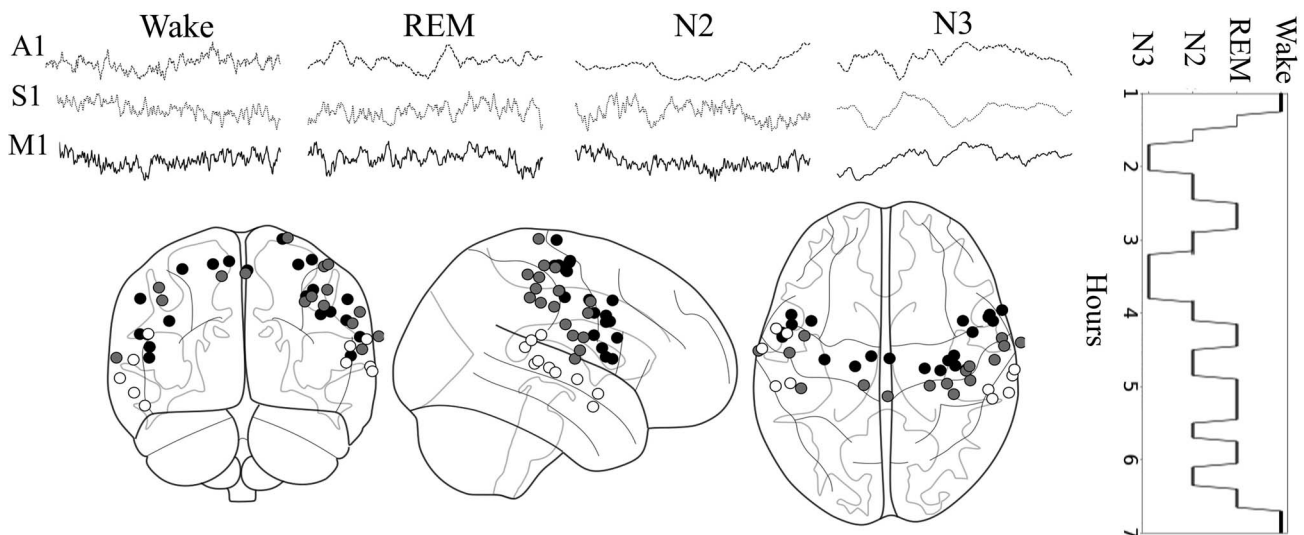
Fig. 2. Tri-dimensional representation of selected representative channels and hypnogram. Representation, in the 3 spatial projections, of the position of the electrode contacts for the analyzed channels in the subjects having data collected in at least 2 ROIs, among A1 (white), S1 (gray), and M1 (black). On top, we represent an example, in one subject, of sEEG time course (2 s long) for the A1 (dashed line), S1 (dotted line), and M1 (continuous line) cortical parcels, in the awake and the 3 studied sleep stages. The amplitude of sEEG in each area is normalized to [−1, 1]. On the right side, a typical hypnogram is shown.

methods for investigating complexity such as box counting, correlation dimension, or Katz algorithm (Accardo et al. 1997).

The HFD algorithm (Higuchi 1988) is based on quantifying the appearance of self-similarities across different time scales. HFD is estimated from the relationship between the length of down-sampled series and the sampling steps. The down-sampling is executed from 2 to k_{max}, and the estimates depend on this single parameter. Although there is no gold standard for the k_{max} selection, we treasured of multiple previous investigations about the HFD dependence from k_{max}, and in the present work we estimated the HFD at the value of k_{max} where HFD starts stabilizing, namely k_{max}=35, in agreement with (Armonaite et al. 2021), across all subjects, ROIs, and states.

Statistical analysis

We observed that both PSD values in each frequency band, and HFD values, across different sleep stages, show a non-Gaussian distribution of population (as it has been confirmed by Shapiro–Wilk test). Thus, in order to compare the PSDs and HFDs of the cortical ROIs, we used the non-parametric Wilcoxon test (hereafter W_{test} values). This test is not applicable to too small populations, therefore only between S1 and M1 sources such quantitative comparison was feasible. However, for the comparison of the latter 2 regions with A1 we provided the Fisher's exact test ($F's_{test}$).

Results

We aim at evaluating the differences of neuronal ongoing activity between distinct primary cortices within a subject. For this purpose, we were restricted to select only the subjects who had recordings in at least 2 of

the ROIs. Hence, the total number of subjects that were inquired in N2 and N3 sleep states is 16, among which the S1—M1 neurodynamics comparisons were viable in 14, the A1—S1 in 4 and the A1—M1 in 6 subjects. Instead in REM sleep, the S1—M1 neurodynamical features' comparisons were realizable in 11 subjects, for A1—S1 in 3 subjects, and for A1—M1 in 5 subjects. Furthermore, we studied these differences of the neuronal ongoing activity between the 3 ROIs across different sleep states.

Neurodynamics—power spectrum density

We found that, while in wakefulness, S1 prevailed in alpha band to M1, and M1 prevailed to S1 in high beta, low gamma, and high gamma. Instead, in REM sleep, M1 had greater power than S1 in low beta, high beta, and low gamma (Fig. 3, Supplementary Fig. 3a, Fig. 4, Supplementary Fig. 4a, and Table 1). In N2 stage, M1 had greater power than S1 in alpha band. In N3 stage, M1 was prevailing to S1 in alpha and theta bands, whereas in delta S1 prevailed to M1.

When comparing A1 with S1 and M1, in resting wakefulness state, we observed that A1 had greater power than S1 and M1 in delta band and lower than S1 and M1 in low beta band. In REM stage, M1 power was prevailing A1 in theta, beta, and gamma bands. In N2 stage, A1 power was higher than S1 in delta band, instead the oppositely from alpha to gamma S1 power prevailed over A1. M1 PSD was observed to be higher than A1 only in low beta band. In N3 sleep stage, A1 power is higher than M1 in delta band and M1 PSD is higher than A1 in theta, alpha, and low beta bands. However, S1 expresses higher power than A1 in low beta high beta and low gamma frequency bands (Table 1).
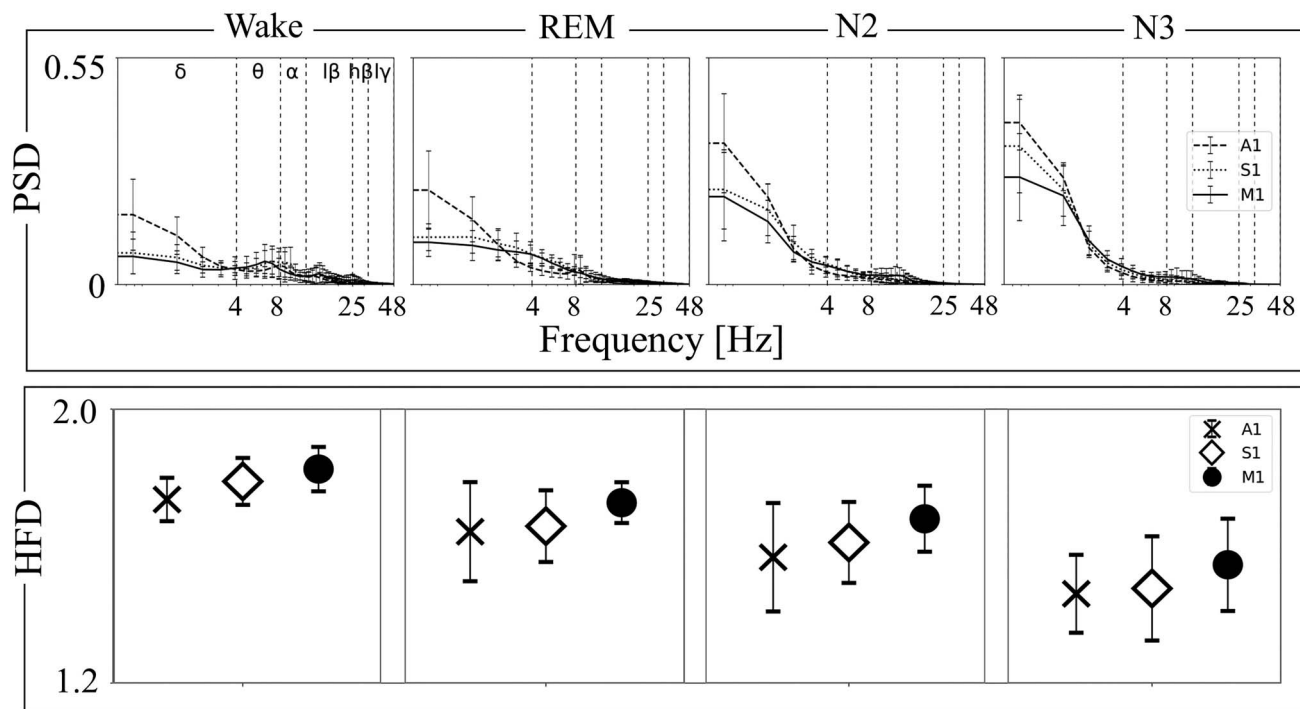
Fig. 3. Spectral and fractal estimation of local neurodynamics across people in wake and sleep. PSD and HDF mean across population in 3 ROIs, in all stages: wake, REM, N2, and N3. In the top panel, the mean and standard deviation of PSD as a function of frequency across all selected subjects, separately for M1, S1, and A1 areas, are presented. PSD values are normalized so that the area under each curve is equal to 1. Frequency band ranges: δ [≤3 Hz], θ [4–7 Hz], α [8–12 Hz], lβ [13–25 Hz], hβ [26–32 Hz], and lγ [33–48 Hz]. Though the comparisons are given in the tables. Bottom panel shows HFD mean and standard deviation across the same population.
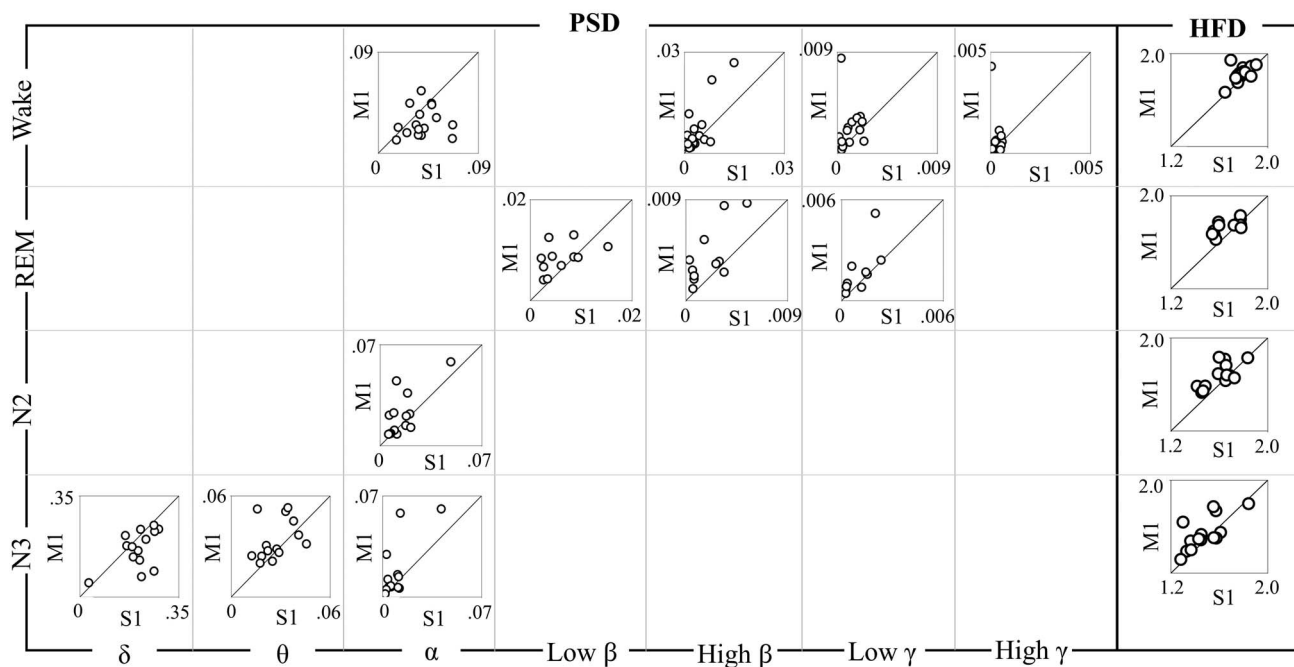
Fig. 4. Intra-subject comparison of M1 vs S1 neurodynamic as featured by PSD and HFD. Left 7-columns rectangle: In awake and the 3 studied sleep stages (rows), intra-subject comparison of the S1's and M1's neurodynamics via the scatterplots of within subject PSD band values for the frequency bands where the S1 differs from M1. Right 1-column rectangle: scatterplots of M1 vs. S1 HFDs. In each plot, a point above (below) the diagonal represents a subject with PSD/HFD value in M1 higher (lower) than in S1.

Table 1. Neurodynamics comparison between cortical parcels.

			PSD							HFD
			δ	θ	α	Low β	High β	Low γ	High γ	
Wake	S1–M1	W_{test}	46	55	**26**	46	**25**	15	**28**	12
		P	0.26	0.50	**0.03** >	0.26	**0.03** <	**0.01** <	**0.04** <	**0.00** <
	A1–S1	$F's_{test}$	**0.00** >	0.99	0.57	**0.08** <	0.57	0.57	0.99	**0.00** <
	A1–M1	$F's_{test}$	**0.00** >	0.35	0.35	**0.06** <	0.35	0.35	0.99	**0.00** <
REM	S1–M1	W_{test}	15	24	18	**11**	**4**	**5**	16	**6**
		P	0.11	0.42	0.18	**0.05** <	**0.01** <	**0.01** <	0.13	**0.02** <
	A1–S1	$F's_{test}$	0.99	0.10	0.99	0.10	0.10	0.10	0.10	0.10
	A1–M1	$F's_{test}$	0.21	**0.01** <	0.99	**0.01** <	**0.01** <	**0.01** <	**0.01** <	0.21
N2	S1—M1	W_{test}	37	49	**24**	34	32	25	27	**16**
		P	0.33	0.83	**0.07** <	0.25	0.20	0.08	0.11	**0.02** <
	A1–S1	$F's_{test}$	**0.03** >	0.49	**0.03** <	**0.03** <	**0.03** <	**0.03** <	**0.03** <	**0.03** <
	A1–M1	$F's_{test}$	0.57	0.57	0.57	**0.08** <	0.57	0.57	0.99	**0.08** <
N3	S1–M1	W_{test}	**22**	**22**	18	36	35	33	35	**24**
		P	**0.06** >	**0.06** <	**0.03** <	0.30	0.27	0.22	0.27	**0.07** <
	A1–S1	$F's_{test}$	0.99	0.99	0.49	**0.03** <	**0.03** <	**0.03** <	0.49	**0.03** <
	A1–M1	$F's_{test}$	**0.08** >	**0.08** <	**0.08** <	**0.08** <	0.57	0.57	0.99	0.57

Note: PSD statistical comparisons between cortical area pairs in awake and sleep states for each frequency band. In the last column, similar statistical analysis for HFD data. Wilcoxon test statistics (W_{test}) and P value are reported for comparing the S1 and M1 regions. Instead, we indicate P value of a Fisher's exact test (notated as $F's_{test}$) for comparisons S1 and M1 with A1. The tag < (>) indicates that the population PSD of the area mentioned as first (S1 or A1) is lower (higher) than the area mentioned as second (M1 or S1). The same symbolic convention is adopted for the HFD comparisons. Statistically significant differences between the compared areas are in bold ($P \leq 0.08$, taking into account the occurring distribution, see Fig. 4 and Supplementary Fig. 4a). We adopted the notation $P = 0.00$, for values $P < 0.005$.

PSD features across different sleep stages and wake state showed the expected changes in each cortical area (Table 2). Power level is higher in wakefulness that N2 sleep (denoted shortly Wake > N2) in higher frequencies (low beta, high beta, low gamma, and high gamma) in both M1 and S1, whereas in theta and alpha bands only in S1; also Wake > REM in low beta band in both M1 and S1, and in alpha in S1; instead, REM, N2 and N3 > Wake in delta frequency band but REM > N2 in the remaining bands. For comparisons in A1 N3 > N2 > Wake and N3 > REM in delta band. Wake > N2 and Wake > N3 in remaining bands, instead N2 > N3 in beta and gamma bands.

Neurodynamics—HFD

In assessing the cortical parcels' neurodynamics we also compared the HFD between the primary cortical ROIs. We observed that M1 HFD was always higher than S1 in N2, N3, and REM sleep stages, consistently with the behavior in wakefulness.

Assessment for A1–S1 and A1–M1 comparison (Table 1) suggests that, across all sleep stages except REM, HFD of S1 is higher than in A1, as well as HFD of M1 is higher than in A1. However, the A1–M1 comparisons in N3 has lacked evidence that the differences would be statistically significant, though 4 subjects out of 6 had higher HFD in M1 than in A1. Comparing the sleep stages and wakefulness in S1 and M1 we spotted out that HFD Wake > REM > N2 > N3, instead in A1 we obtained HFD Wake > N2 > N3 and REM > N2 (Table 2).

Discussion

The key result of our study is that, despite the huge neurodynamical changes in awake and diverse sleep stages, the neurodynamics of a single subject of each cortical parcel differs from another cortical parcel in all these conditions. That is, the local neurodynamics distinctive features persist to the revolution within the brain activity that sleep induces.

Fractal vs. spectral features

In awake, the differentiation between areas assessed via the HFD corresponded to a wide differentiation of the PSD values. During sleep, the neurodynamics assessed via HFD complexity measure clearly and stably differed in diverse primary cortical parcels in awake and all sleep stages. Recognizing a rule of PSD differences among these areas, M1 prevailed with respect to S1 and A1 in the higher frequency bands: from awake (where gamma is present and M1 prevails in beta and gamma) till to N3, where highest frequency is alpha and it prevails in theta and alpha.

Neurodynamics complexity reduction from wake to deep sleep

The ability to process information is modulated by the sleep cycles. In awake, higher functional activation corresponds to higher complexity as sensed by higher fractal dimension. This occurs not only when passing from resting state with closed eyes to resting state with open eyes, or with somatosensory stimulations, or with actively executing a movement (Cottone et al. 2017), but also when the cognitive process becomes more demanding (Ma et al. 2018; Ruiz de Miras et al. 2019). When the behavioral state goes to complete relaxation, the complexity reduction of neurodynamics parallels, at neuronal network level, the overall synchronization across wide brain areas. When sleep enters deeper stages,

Table 2. Neurodynamics comparison between sleep stages.

			PSD							HFD
			δ	θ	α	Low β	High β	Low γ	High γ	
M1	Wake—N2	W_{test}	1	34	40	5	7	11	17	2
		P	**0.00 <**	0.08	0.15	**0.00 >**	**0.00 >**	**0.00 >**	**0.01 >**	**0.00 >**
	Wake—N3	W_{test}	0	31	20	0	0	3	7	0
		P	**0.00 <**	0.06	**0.01 >**	**0.00 >**	**0.00 >**	**0.00 >**	**0.00 >**	**0.00 >**
	Wake—REM	W_{test}	11	29	23	15	22	23	23	3
		P	**0.02 <**	0.25	0.12	**0.03 >**	0.10	0.12	0.12	**0.00 >**
	N2—N3	W_{test}	7	42	17	0	0	0	0	0
		P	**0.00 <**	0.18	**0.01 >**	**0.00 >**	**0.00 >**	**0.00 >**	**0.00 >**	**0.00 >**
	REM—N2	W_{test}	1	1	16	2	0	0	0	0
		P	**0.00 <**	**0.00 >**	**0.04 >**	**0.00 >**	**0.00 >**	**0.00 >**	**0.00 >**	**0.00 >**
	REM—N3	W_{test}	0	1	1	0	0	0	0	0
		P	**0.00 <**	**0.00 >**	**0.00 >**	**0.00 >**	**0.00 >**	**0.00 >**	**0.00 >**	**0.00 >**
S1	Wake—N2	W_{test}	1	20	4	12	11	13	17	2
		P	**0.00 <**	**0.04 >**	**0.00 >**	**0.01 >**	**0.01 >**	**0.01 >**	**0.03 >**	**0.00 >**
	Wake—N3	W_{test}	1	5	1	3	10	6	10	1
		P	**0.00 <**	**0.00 >**	**0.00 >**	**0.00 >**	**0.01 >**	**0.00 >**	**0.01 >**	**0.00 >**
	Wake—REM	W_{test}	5	16	2	12	14	26	21	4
		P	**0.01 <**	0.13	**0.01 >**	**0.06 >**	0.09	0.53	0.29	**0.01 >**
	N2—N3	W_{test}	0	3	1	0	14	9	4	1
		P	**0.00 <**	**0.00 >**	**0.00 >**	**0.00 >**	**0.02 >**	**0.01 >**	**0.00 >**	**0.00 >**
	REM—N2	W_{test}	0	2	5	9	8	7	6	7
		P	**0.00 <**	**0.01 >**	**0.01 >**	**0.03 >**	**0.03 >**	**0.02 >**	**0.02 >**	**0.02 >**
	REM—N3	W_{test}	0	0	1	1	0	0	0	1
		P	**0.00 <**	**0.00 >**	**0.00 >**	**0.00 >**	**0.00 >**	**0.00 >**	**0.00 >**	**0.00 >**
A1	Wake—N2	F'_{test}	**0.00 <**	**0.08 >**	**0.00 >**	**0.00 >**	**0.00 >**	**0.08 >**	**0.08 >**	**0.00 >**
	Wake—N3	F'_{test}	**0.00 <**	**0.08 >**	**0.00 >**	**0.00 >**	**0.00 >**	**0.00 >**	**0.00 >**	**0.00 >**
	Wake—REM	F'_{test}	0.99	0.99	0.21	0.21	0.99	0.99	0.99	0.21
	N2—N3	F'_{test}	**0.08 <**	0.57	0.57	**0.08 >**	**0.08 >**	**0.08 >**	**0.08 >**	**0.08 >**
	REM—N2	F'_{test}	0.21	0.99	0.21	0.21	0.21	0.21	0.21	0.21
	REM—N3	F'_{test}	**0.01 <**	0.21	**0.01 >**	**0.01 >**	**0.01 >**	**0.01 >**	**0.01 >**	**0.01 >**

Note: PSD statistical comparisons between wake and sleep states pairs, for each cortical ROI and frequency band. In the last column, similar statistical analysis for HFD data. As in Table 1 the statistics performed by Wilcoxon test for the S1–M1 comparison and Fisher's exact test for A1, as well as the same notations for direction of changes and P values was applied. Statistically significant values are in bold ($P \le 0.08$). We adopted the notation $P = 0.00$ for values $P < 0.005$.

neurons become widely synchronized in delta range (Borbely 1982; Ahmed and Cash 2013).

The modulation of complexity during sleep emerged clearly using HFD in the whole cortical mantle, with overall frontal areas displaying higher complexity than postcentral areas in all sleep stages in average on the population. (Olejarczyk et al. 2022). This strengthens our result of within-subject specificity of the local neurodynamics. Furthermore, the selection of primary motor and primary somatosensory areas allows investigating the crucial interplay between these 2 counterparts, implementing the feedback mechanisms mandatory for motor control (Tecchio et al. 2007; Fink et al. 2014), as modified by sleep phenomena.

Higher motor than sensory and auditory cortices complexity—from awake resting state to sleep insight

Higher complexity of M1 neurodynamics with respect to S1 and A1 could be explained by the anatomical structures of these cortices. The frontal lobe neuronal pools are more densely connected than the parietal or temporal lobes (Modha and Singh 2010), so that we can

hypothesize that the complexity of the neuronal activity emerges from the level of local neuronal connectivity.

From the point of view of network physiology (Buzsáki and Draguhn 2004; Sporns and Betzel 2016) the nodes of neuronal networks with highly interconnected hub nature are expected to express an activity with higher complexity. This is exemplified by the primary motor cortex, the very last station of all neuronal networks, as the station origin of the signals dispatched to all muscular effectors (Rizzolatti and Luppino 2001). Applying the same principle, the primary somatosensory nodes are expected to be characterized by activity of greater complexity than the primary auditory areas, as they constitute 30% of the fibers' origin of the corticospinal tract (Seo and Jang 2013), hence they are constitutive component of the feedback loop that controls any behavior performed (Fink et al. 2014). That is, the level of complexity of the neurodynamics with M1 > S1 > A1 well fits the network physiology expectations.

Limitation of the study

A main limitation of present investigation concerns the nature of sEEG signals analyzed, coming from subjects

diagnosed with severe epilepsy. Although scalp EEGs in wakefulness for healthy subjects have been extensively investigated (Jurcak et al. 2007), the literature of analyses of intracranial EEG activity in healthy subjects is scarce. Subjects with refractory focal epilepsies are the only where extensive intracranial sEEG studies are carried out, that allows studying both pathological and normal brain cortical areas. The MNI Atlas is the first database of "spared regions" intracranial sEEG. Each of the sEEG channel from MNI Atlas—adopted in the present study—is classified as "normal" only if satisfies very restrictive selection criteria. In these bases, we can report behavior related to "normal" areas, although aware of epilepsy as a network pathology given the core characteristics of altered connectivity patterns between epileptogenic areas and the structures linked to them (Bettus et al. 2009; Pittau et al. 2012; Tecchio et al. 2018). Furthermore, the sample herein analyzed presented non-homogeneous characteristics in relation to age (from 13 to 68 years old). This feature is expected to generate part of the variability in the local neurodynamics. In fact, in the life span of healthy subjects, the brain complexity hugely modifies both structurally (Marzi et al. 2020) and functionally (Zappasodi et al. 2015; Smits et al. 2016).

A clear limitation of the study is also the small available dataset. This was determined by the non-uniform distribution of available channels across subjects together with the requirement to assess diverse cortical regions in the same subject.

Individual neurodynamics—investigation dataset as output of the present work

A relevant output of our work is the selection from the world-wide accessible MNI intracranial sEEG database of intra-individual primary cortical parcels data. This allows to quantify local neurodynamics as well as functional connectivity. The possibility to investigate, within a subject, neurodynamics of cortical parcels, in all the sleep phases, constitutes a step forward for studying the vital role that sleep plays in the organization of the neuronal, hormonal, and immune systems. The ability to investigate in well-selected representatives, within paradigmatic cortical parcels of the same person, neuronal network features of single nodes and their connectivity fits well with the EU strategy aiming at building through the EBRAINS (https://ebrains.eu/), funded by the Human Brain Project flagship, a crucial tool for neuroscientific integration of multilevel investigations, enabling advancements for social economic and community's benefits.

In conclusion, our work further strengthens the study of the neurodynamics properties of local neuronal networks' nodes as a result of their structure and functional role within the brain hierarchy. A possible impact of this analysis mainly relates the potential to customize the communication with the brain in the case of interventions for mitigating behavior disorders

and more in general in neuromodulation. In fact, neuromodulation—techniques that modify the excitability of the neural target thus changing its relationship with the connected areas and consequently its function—emerge more and more consistently able to relief eating disorders and addiction (Song et al. 2021), depression and chronic fatigue (Brunoni et al. 2016; Gianni et al. 2021). In a seminal non-invasive transcranial electric stimulation (tES) study, the authors of (Cottone et al. 2018) proved that a current which mimics the endogenous dynamics of the target neuronal pools, neuromodulates more efficiently than the sinusoid at a locally-tuned frequency, suggesting that structured patterns transmit entrainment more than a non-structured stationary signal (Réboli et al. 2022). The investigation carried out in the present analysis paves the way of further neuromodulation personalization, as the knowledge on local neurodynamics allows better tuning the neuromodulation to the desired neuronal pool target and obtaining higher efficacy in compensating symptoms secondary to alterations of the neurodynamics, like depression, addiction, pain, and fatigue. On the other side, given the deep interrelation between mental behavioral disorders and sleep disturbances (Wittchen et al. 2011), we believe that neuromodulations reducing the behavior alterations (Gianni et al. 2021; Song et al. 2021) could result in sleep rebalance. Since non-invasive neuromodulation can be applied during sleep, further knowledge on neurodynamics properties during sleep can be exploited to deliver the stimulation also in these physiological states.

Supplementary material

Supplementary material is available at *Cerebral Cortex* online.

References

Accardo A, Affinito M, Carrozzi M, Bouquet F. Use of the fractal dimension for the analysis of electroencephalographic time series. *Biol Cybern*. 1997:77(5):339–350.

Ahmed OJ, Cash SS. Finding synchrony in the desynchronized EEG: the history and interpretation of gamma rhythms. *Front Integr Neurosci*. 2013:7:1–7.

Andrillon T, Poulsen AT, Hansen LK, Léger D, Kouider S. Neural markers of responsiveness to the environment in human sleep. *J Neurosci*. 2016:36(24):6583–6596.

Armonaite K, Bertoli M, Paulon L, Gianni E, Balsi M, Conti L, Tecchio F. Neuronal electrical ongoing activity as cortical areas signature: an insight from MNI intracerebral recording atlas. *Cereb Cortex*. 2021. https://doi.org/10.1093/cercor/bhab389.

Axmacher N, Mormann F, Fernández G, Elger CE, Fell J. Memory formation by neuronal synchronization. *Brain Res Rev*. 2006:52(1): 170–182.

Bettus G, Guedj E, Joyeux F, Confort-Gouny S, Soulier E, Laguitton V, Cozzone PJ, Chauvel P, Ranjeva JP, Bartolomei F, Guye M. Decreased basal fMRI functional connectivity in epileptogenic networks and contralateral compensatory mechanisms. *Hum Brain Mapp*. 2009:30(5):1580–1591. https://doi.org/10.1002/hbm.20625.

Borbely AA. A two process model of sleep regulation. *Hum Neurobiol*. 1982:1(3):195–204.

Brunoni A, Nitsche M, Loo C. Transcranial direct current stimulation in neuropsychiatric disorders: clinical principles and management. *Transcranial Direct Curr Stimul Neuropsychiatr Disord Clin Princ Manag*. 2016:1–414.

Burioka N, Miyata M, Cornélissen G, Halberg F, Takeshima T, Kaplan DT, Suyama H, Endo M, Maegaki Y, Nomura T, et al. Approximate entropy in the electroencephalogram during wake and sleep. *Clin EEG Neurosci*. 2005:36(1):21–24.

Buzsáki G, Draguhn A. Neuronal olscillations in cortical networks. *Science*. 2004:304(5679):1926–1929.

Casali AG, Gosseries O, Rosanova M, Boly M, Sarasso S, Casali KR, Casarotto S, Bruno MA, Laureys S, Tononi G, et al. A theoretically based index of consciousness independent of sensory processing and behavior. *Sci Transl Med*. 2013:5(198):198ra105.

Collantoni E, Madan CR, Meneguzzo P, Chiappini I, Tenconi E, Manara R, Favaro A. Cortical complexity in anorexia nervosa: a fractal dimension analysis. *J Clin Med*. 2020:9(3):833.

Cottone C, Porcaro C, Cancelli A, Olejarczyk E, Salustri C, Tecchio F. Neuronal electrical ongoing activity as a signature of cortical areas. *Brain Struct Funct*. 2017:222(5):2115–2126.

Cottone C, Cancelli A, Pasqualetti P, Porcaro C, Salustri C, Tecchio F. A new, high-efficacy, noninvasive transcranial electric stimulation tuned to local neurodynamics. *J Neurosci*. 2018:38(3):586–594.

Croce P, Quercia A, Costa S, Zappasodi F. Circadian rhythms in fractal features of EEG signals. *Front Physiol*. 2018:9:1567.

Fink AJP, Croce KR, Huang ZJ, Abbott LF, Jessell TM, Azim E. Presynaptic inhibition of spinal sensory feedback ensures smooth movement HHS public access. *Nature*. 2014:509(7498):43–48.

Frauscher B, von Ellenrieder N, Zelmann R, Rogers C, Nguyen DK, Kahane P, Dubeau F, Gotman J. High-frequency oscillations in the normal human brain. *Ann Neurol*. 2018:84(3):374–385.

Gent TC, Bandarabadi M, Herrera CG, Adamantidis AR. Thalamic dual control of sleep and wakefulness. *Nat Neurosci*. 2018:21(7): 974–984.

Gianni E, Bertoli M, Simonelli I, Paulon L, Tecchio F, Pasqualetti P. tDCS randomized controlled trials in no-structural diseases: a quantitative review. *Sci Rep*. 2021:11(1):16311.

Gorgoni M, Sarasso S, Moroni F, Sartori I, Ferrara M, Nobili L, De Gennaro L. The distinctive sleep pattern of the human calcarine cortex: a stereo-electroencephalographic study. *Sleep*. 2021:44(7): 1–10.

Higuchi T. Approach to an irregular time series on the basis of the fractal theory. *Physica D: Nonlinear Phenomena*. 1988:31(2):277–283.

Jurcak V, Tsuzuki D, Dan I. 10/20, 10/10, and 10/5 systems revisited: their validity as relative head-surface-based positioning systems. *Neuroimage*. 2007:34(4):1600–1611. https://doi.org/10.1016/j.neuroimage.2006.09.024.

Klonowski W. Chaotic dynamics applied to signal complexity in phase space and in time domain. *Chaos, Solitons Fractals*. 2002:14(9):1379–1387.

Lopes Da Silva FL. *Niedermeyer's electroencephalography: basic principles, clinical applications and related fields*. 6th ed. Philadelphia: Lippincott Williams & Wilkins; 2011

Ma Y, Shi W, Peng CK, Yang AC. Nonlinear dynamical analysis of sleep electroencephalography using fractal and entropy approaches. *Sleep Med Rev*. 2018:37:85–93.

Marino M, Liu Q, Samogin J, Tecchio F, Cottone C, Mantini D, Porcaro C. Neuronal dynamics enable the functional differentiation of resting state networks in the human brain. *Hum Brain Mapp*. 2019:40(5):1445–1457.

Marzi C, Marco G, Carlo T, Mario M, Stefano D. Toward a More Reliable Characterization of Fractal Properties of the Cerebral Cortex of Healthy Subjects during the Lifespan. *Scientific Reports*. 2020:10(1): 16957. https://doi.org/10.1038/s41598-020-73961-w.

Modha DS, Singh R. Network architecture of the long-distance pathways in the macaque brain. *Proc Natl Acad Sci U S A*. 2010:107(30): 13485–13490.

Moruzzi G, Magoun HW. Brain stem reticular formation and activation of the EEG. *Electroencephalogr Clin Neurophysiol*. 1949:1(1–4): 455–473.

Nobili L, Ferrara M, Moroni F, De Gennaro L, Lo RG, Campus C, Cardinale F, De Carli F. Dissociated wake-like and sleep-like electro-cortical activity during sleep. *NeuroImage*. 2011:58(2): 612–619.

Olejarczyk E, Gotman J, Frauscher B. Region-specific complexity of the intracranial EEG in the sleeping human brain. *Sci Rep*. 2022:12(1):451.

Pittau F, Grova C, Moeller F, Dubeau F, Gotman J. Patterns of altered functional connectivity in mesial temporal lobe epilepsy. *Epilepsia*. 2012:53(6):1013–1023. https://doi.org/10.1111/j.1528-1167.2012.03464.x.

Réboli LA, Maciel RM, de Oliveira JC, Moraes MFD, Tilelli CQ, Cota VR. Persistence of neural function in animals submitted to seizure-suppressing scale-free nonperiodic electrical stimulation applied to the amygdala. *Behav Brain Res*. 2022:426:113843.

Rizzolatti G, Luppino G. The cortical motor system. *Neuron*. 2001:31(6):889–901.

Ruiz de Miras J, Soler F, Iglesias-Parro S, Ibáñez-Molina AJ, Casali AG, Laureys S, Massimini M, Esteban FJ, Navas J, Langa JA. Fractal dimension analysis of states of consciousness and unconsciousness using transcranial magnetic stimulation. *Comput Methods Prog Biomed*. 2019:175:129–137.

Schartner MM, Pigorini A, Gibbs SA, Arnulfo G, Sarasso S, Barnett L, Nobili L, Massimini M, Seth AK, Barrett AB. Global and local complexity of intracranial EEG decreases during NREM sleep. *Neurosci Conscious*. 2020:2017:1–12.

Seo JP, Jang SH. Different characteristics of the corticospinal tract according to the cerebral origin: DTI study. *Am J Neuroradiol*. 2013:34(7):1359–1363.

Smits FM, Porcaro C, Cottone C, Cancelli A, Rossini PM, Tecchio F. Electroencephalographic Fractal Dimension in Healthy Ageing and Alzheimer's Disease. *PLoS One*. 2016:11(2):e0149587. https://doi.org/10.1371/journal.pone.0149587.

Song S, Zilverstand A, Gui W, Pan X, Zhou X. Reducing craving and consumption in individuals with drug addiction, obesity or overeating through neuromodulation intervention: a systematic review and meta-analysis of its follow-up effects. *Addiction*. 2021:117(5):1242–1255.

Sporns O, Betzel RF. Modular brain networks. *Annu Rev Psychol.* 2016:67(1):613–640.

Steinman L. Elaborate interactions between the immune and nervous systems. *Nat Immunol.* 2004:5(6):575–581.

Steriade M, McCormick DA, Sejnowski TJ. Thalamocortical oscillations in the sleeping and aroused brain. *Science.* 1993:262(5134):679–685.

Tecchio F, Graziadio S, Barbati G, Sigismondi R, Zappasodi F, Porcaro C, Valente G, Balsi M, Rossini PM. Somatosensory dynamic gamma-band synchrony: a neural code of sensorimotor dexterity. *NeuroImage.* 2007:35(1):185–193.

Tecchio F, Cottone C, Porcaro C, Cancelli A, Di Lazzaro V, Assenza G. Brain Functional Connectivity Changes After Transcranial Direct Current Stimulation in Epileptic Patients. *Front Neural Circuits.* 2018:12:44. https://doi.org/10.3389/fncir.2018.00044.

von Ellenrieder N, Gotman J, Zelmann R, Rogers C, Nguyen DK, Kahane P, Dubeau F, Frauscher B. How the human brain sleeps: direct cortical recordings of normal brain activity. *Ann Neurol.* 2020:87(2):289–301.

Wittchen HU, Jacobi F, Rehm J, Gustavsson A, Svensson M, Jönsson B, Olesen J, Allgulander C, Alonso J, Faravelli C, et al. The size and burden of mental disorders and other disorders of the brain in Europe 2010. *Eur Neuropsychopharmacol.* 2011:21(9):655–679.

Zappasodi F, Marzetti L, Olejarczyk E, Tecchio F, Pizzella V. Age-Related Changes in Electroencephalographic Signal Complexity. *PLoS One.* 2015:10(11):e0141995. https://doi.org/10.1371/journal.pone.0141995.

Zhang X, Lei B, Yuan Y, Zhang L, Hu L, Jin S, Kang B, Liao X, Sun W, Xu F, et al. Brain control of humoral immune responses amenable to behavioural modulation. *Nature.* 2020:581(7807):204–208.